Journal of Neonatal Surgery
ISSN(Online): 2226-0439
Vol. 13, (2024)
https://www.jneonatalsurg.com

OPEN ACCESS

Ascorbic acid sensor based on ZnO/B(PM-PA) nanocomposite

P. Pon Maha lakshmi[1,2], P. Rajakani[*2], C.Vedhi[2]

[1]Research Scholar, Reg. No:21112232032007, Affiliated by Manonmaniam Sundaranar University, Abishekapatti, Tirunelveli - 627 012, Tamil Nadu, India.

[2]PG and Research Department of Chemistry, V. O. Chidambaram College, Tuticorin - 628 008, Tamil Nadu.

***Correspondence Author:**

Email ID: prkvoc@gmail.com

Cite this paper as: P. Pon Maha lakshmi, P. Rajakani, C.Vedhi, (2024) Ascorbic acid sensor based on ZnO/B(PM-PA) nanocomposite. *Journal of Neonatal Surgery*, 13, 652-661.

ABSTRACT

Recent years have seen a rise in interest in polymer nanocomposites based on electroactive conducting polymers with nanoparticle fillers because of their highly desirable multifunctional characteristics. A precise and considerate evaluation of AA is essential in the diagnosis of several mental disorders. Determining its presence in biological samples is still challenging since it coexists with other high-concentration biomolecules. We introduce a facile, eco-friendly Sensor B(PM-PA) Polymer blend (PB) and ZnO/B(PM-PA) nanocomposite (NCP). Analytical methods, including FT-IR, XRD analysis, and UV-Vis, were employed to explain these nanocomposites. A novel B(PM-PA)/ ZnO electrochemical biosensor was introduced for the in vivo detection of ascorbic acid. In addition, the electrocatalytic reduction of AA on PB&NCP was briefly investigated and achieved good analytical performance with an excellent linear range (0.03-0.1 µM), and a low detection limit (1.14mM&0.44µM). Therefore, the finding of PB&NCP nanocomposite can be regarded as an effective catalyst to enhance the AA detection.

Keywords: *PMMA, PANI, ZnO, Ascorbic acid detection, ZnO/(PM-PA) nanocomposites.*

1. INTRODUCTION

Polymer nanocomposites could offer enormous future possibilities for many materials by resolving various issues and everyday challenges in the current world. As effective materials for sensing applications, nanocomposites have been used. The sensing characteristics of nanoparticles are significantly influenced by their chemical structure [1]. A variety of polymers from the conducting polymer, thermoplastic, elastomer, and other categories have been employed in the case of polymer nanocomposites. The majority of conjugated polymers utilized in sensing applications include conducting blends, polyaniline, polypyrrole, and polythiophene. By improving the electrical conductivity and percolation properties of the nanomaterials, the incorporation of nanoparticles into conducting polymers has further improved the sensors' performance. [2]Nevertheless, a variety of non-conductive polymers have also been used to create sensor nanomaterials.[3]Adding nanoparticles to a polymer matrix to generate nanofilled polymer composites can greatly enhance performance by simply utilizing the characteristics, nature of the nanoscale filler, and flexural mechanical properties.[4-6].In response to a variety of analytes, ions, and molecules, the nanocomposite sensors demonstrated outstanding molecular recognition sensitivity and responsiveness. [7]Thus, polymethyl methacrylate (PMMA) is a viable option for gas sensing because of its unique electrical and physicochemical properties, manufacturing simplicity, and room temperature activity.[8] One of the most extensively researched conducting polymers, polyaniline (PANI), has attracted a lot of interest in the development of electrochemical transducers because of its high electrical conductivity.[9]The total sensor performance may also be further enhanced by including nanomaterials like graphene, carbon nanotubes, gold nanoparticles, etc., inside the PANI matrix due to their exceptional physicochemical properties and synergistic interactions. [10-12] Zinc oxide (ZnO) has attracted special interest due to its exceptional qualities of high catalytic activity, non-toxicity, and excellent chemical stability. Applications for ZnO nanostructures have been investigated during the past few decades, including solar cells, gas sensors, piezoelectric nanogenerators, field effect transistors, and cold cathode electron sources.[13]

Application for Ascorbic acid electrochemical biosensing. In this situation, electrochemical techniques are more appropriate, dependable, cost-effective, and practical for field use. The electrochemical methods provide remarkable reproducibility, precision, and low detection limits, together with linear wide-range responses [14] Ascorbic acid (AA) has several physiological and pharmacological roles in drug metabolism, intestinal absorption of iron, and collagen formation.

Additionally, ascorbic acid has been studied in connection with mental disease, infertility, and cancer, as well as for the prevention and treatment of the common cold.[15-17]

Considering the aforementioned discussion, the main goal of this study is to create new B(PM-PA)/ZnO nanocomposite-modified sensor platforms for rapid ascorbic acid detection. The specific tasks include: (i) synthesizing and systematically characterizing B(PM-PA)/ ZnO nanocomposites using a variety of spectroscopic and microscopic techniques; (ii) fabricating and testing chemically modified electrodes electrochemically; and (iii) determining analytical performance characteristics like the ascorbic acid limit of detection. It is hoped that the basic knowledge acquired from this research will help optimize materials for tunable nanocomposite construction to create highly effective electrochemical detectors. The suggested sensing system is expected to offer an affordable yet efficient analytical tool to detect ascorbic acid.

2. EXPERIMENTAL WORK

2.1. Materials used

Methyl methacrylate(MMA) was purchased from Sigma-Aldrich, Potassium persulfate($K_2S_2O_8$),Sodium dodecyl sulfate (SDS),Aniline,hydrochloric acid,potassium dichromate($K_2Cr_2O_7$),Zinc oxide (ZnO),Ascorbic acid were all acquired from Merck.Chloroform and distilled water were used in the synthesis process.

2.2. Working electrode preparation

In our present investigation, a glassy carbon electrode modified with PB was used. It was made into PB solution by dissolving it in chloroform. Casting a single drop of PB solutions onto a surface and allowing the solvent to evaporate produced PB film. They were consequently rinsed with water and then transferred to an electrochemical cell for experimental purposes. A saturated calomel reference electrode (SCE), platinum wire counter electrode, and glassy carbon working electrode modified via PB were used in a three-electrode cell. Cyclic voltammogram of the PB-modified GCE immersed in 1.0 M H_2SO_4 at 27±2°C for 2 s. Differential pulse voltammetry(DPV) was analyzed in Ascorbic acid detection. The above procedure is followed by NCPs composites.

2.3. Methods

FT-IR spectra of the B(PM-PA)& ZnO /B(PM-PA) nanocomposites were recorded using a Nicolet iS5 FT-IR instrument in the frequency range of 400 to 4000 cm^{-1}. UV-Vis spectra of the solid samples were recorded on a JASCOV630 in the wavelength region 200 to 900nm. Powder X-ray diffraction patterns of the coatings were obtained by employing an XPERT-PRO diffractometer using CuKα(kα= 1.54060Å) radiation. The diffractometer was operated at 45kV and 30mA. Cyclic voltammetry studies were carried out at different pH, and DPV was also experimented with using a CH Instrument(Model 650C) Electrochemical workstation.

2.3.1. Polymerization of MMA

A simple procedure was followed to prepare PMMA, which involved placing 0.1M of MMA, 0.01M of SDS was added in 60 ml of distilled water in a 250ml round bottom flask, and the solution that stirred for 1h at 75˚C. 0.001M of $K_2S_2O_8$ (initiator) dissolved in water was added gradually, drop by drop, and stirred for ½ hour at 80˚C. The solution was then filtered, washed, and finally dried at 100˚C for 24h under vacuum to yield PMMA solid material.

2.3.2.Polymerization of aniline

A mixture of 0.1M of aniline and 1M of HCl was stirred for 3h. 0.1M of $K_2Cr_2O_7$ was added and stirred for about 1 hour in an ice bath, and the precipitated product was collected and washed with distilled water. The synthesized polymer was then dried at 60˚C in a vacuum oven.

2.3.3.Synthesis of B(PM-PA)

PMMA and PANI 2:1 ratio was dissolved in chloroform as a common solvent of both. The two polymers were mixed using a magnetic stirrer for about 4h at 60 ˚C to give a homogeneous solution of a blend of B(PM-PA).

2.3.4.Synthesis of ZnO/B(PM-PA)

To the aforementioned solution, amounts of 0.2 g(NCP) wt% of ZnO were added and stirred for about ½ hour at room temperature. The final solution ZnO/B(PM-PA)was cast in Petri dishes and kept drying at 80˚Cin a vacuum to obtain the nanocomposite.

3. RESULTS AND DISCUSSION

3.1. FT-IR Studies

The results of FT-IR show that the PB and NCP analyzed in the wavenumber range of 4000 to 500 cm^{-1} are shown in Fig. 1.

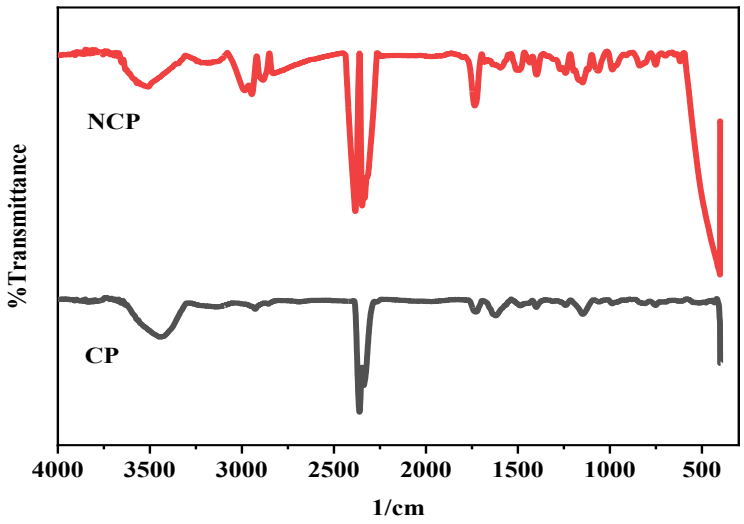

Fig.1.FT-IR behavior of PB and NCP

The peaks resulting from PANI's -NH stretching are at 3443 cm^{-1} [18] and show at the copolymer. The distinct bands of PMMA 1398 cm^{-1} [20] & 1435 cm^{-1} [21] in the NCP IR spectra show the -CH2 twisting and symmetric deformation vibration of the CH3 group. The alkene of PMMA, the copolymer, has a band at 986 cm−1 of (-CH2)n with greater equation ≥4 [18]. Furthermore, at 1734 cm^{-1}, 1241 cm^{-1}, and 1147 cm^{-1} [18], respectively, copolymer and nanocomposite were detected that are attributed to the C=O stretching vibration, C-O-C stretching vibration, and (-OCH3) stretching of PMMA. The observed peak at 842 cm^{-1} corresponds to the long polymeric chain bending in the polymer[22] The PANI peaks at 1581 cm^{-1} and 1363 cm^{-1} are shifted to 1594 cm^{-1}, 1480 cm^{-1}, and 1399 cm^{-1}, respectively. These peak shifts characteristic of PANI nanocomposite may be due to the formation of interactions between the chains of PANI and Zn[22] Moreover, the existence of two peaks at 618 cm^{-1}related to Zn-N stretching frequency and the interaction bond between ZnO and PMMA/PANI chain[23] In addition to the peaks mentioned above, a peak at 430 cm^{-1} that is associated with the Zn-O stretching mode is seen in the successful ZnO/P(MMA-ANI) nanocomposites [23]. The patterns show that adding ZnO nanoparticles to nanocomposites increases absorption intensity because of the uniform dispersion of ZnO nanoparticles in the matrix of the nanocomposite and the removal of agglomeration.[23]

3.2. UV-VIS Spectroscopy studies

UV–Vis spectra were recorded between 200-900nm for the synthesized PB and NCP. Fig. 2 shows UV–VIS absorption spectra of different amounts of ZnO doped with B(PM-PA).

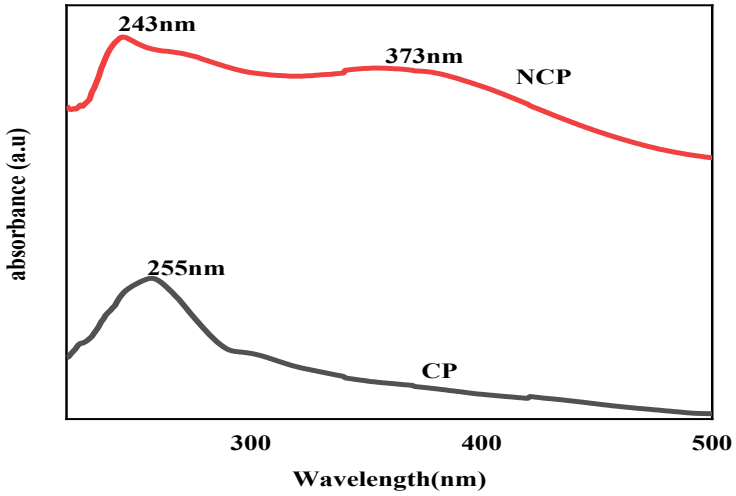

Fig.2.UV–VIS spectra of BP&NCP

Its characteristic band at about 255 nm may be attributed to π → π* which comes from C=O and is observed in FTIR at about 1734 cm−1 [20]. The peaks shift towards smaller wavelengths to 243 nm and 373 nm for ZnO doping B(PM-PA).

3.3. XRD studies

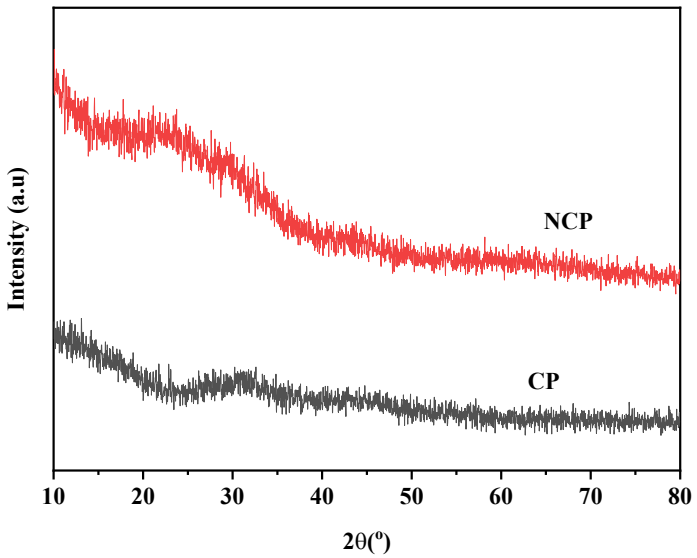

Fig.3 XRD pattern of PB and NCP

The X-ray powder diffraction patterns can be used to analyze the crystal structure, dislocation, strain, and crystal size. XRD patterns of CP and NCP are shown in Fig. 3

The broad peaks 31 ˚-33 ˚ as predicted by confirming the incorporation of PMMA&PANI revealing the copolymer.[24] The different peaks of ZnO /B(PM-PA) at around (2θ) =27˚,31˚, 66˚ and 76˚ of ZnO crystal planes (102) (402) (624) and (1513) respectively.The XRD pattern of ZnO/B(PM-PA) isshown in the orthorhombic structure.These values and structure are matched and confirmed with the reference XRD pattern (JCPDS file no: 96-720-4199).The presence of amorphous B(P(M-PA) reduces the doping with ZnO.

Using Scherrer's formula (Eq. 1), the average crystallite sizes (D) of the nanocomposite were calculated.

$D = 0.9\ \lambda / \beta \cos\theta$ ———————— (1)

Where ‘λ’ is the incoming X-ray beam's wavelength (1.5406Å), ‘β’ is the full width at half maximum value, and ‘ɵ’is the diffraction angle.

Crystallographic defects or dislocations disrupt the regular patterns of crystal lattices. The equation (Eq. 2) may be used to calculate the generated dislocation density (δ).

$\delta = 1 / D^2\ m^{-2}$ ———(2)

The relationship (Eq. 3) may be used to compute the strain (ε) created in the nanocomposite.

$\varepsilon = \beta / 4\tan\theta$ ——— (3)

Table. 1 shows that when ZnO doping, the average crystallite size also increases. This indicates reduces the dislocation density, increasing electrical conductivity,[45] and the strain values vary as well.

Table 1

System	Crystalline size ‘d’ [nm]	Dislocation density$\times 10^{18}[m^{-2}]$	Strain$\times 10^{-3}$
CP	Amorphous	------	------
NCP	11	0.0073	0.0243

3.4. Electrochemical characterization

Cyclic voltammetry

A three-electrode cell with coated glassy carbon (GC) as the working electrode, Ag/AgCl electrode as the reference electrode, and platinum wire as the auxiliary electrode was used to record cyclic voltammograms at ambient temperature. The nanocomposite was placed on the GC working electrode and scanned between 50 and 500 mV/s between -1.0 and 1.4V. As a result of many variables in the experiment, including changing ZnO concentration, pH 1-13, various atmospheres, and scan rate, the voltammetric response was examined for charge transfer found in NCP-coated GCE..

3.4.1.Effect of pH

The Polymer blend and Nanocomposite in aqueous conditions are highly pH-dependent. [25]Therefore, using pH buffer solutions that were adjusted to the required condition, the impact of pH on the voltammetric response was examined at the PB&NCP modified GCE in the range of pH 1.0 to 13.0 as shown in Fig. 4&5.Since pH 1.0 appears to be the ideal pH range for optimal sensitivity response, therefore pH 1.0 is used for the following studies.

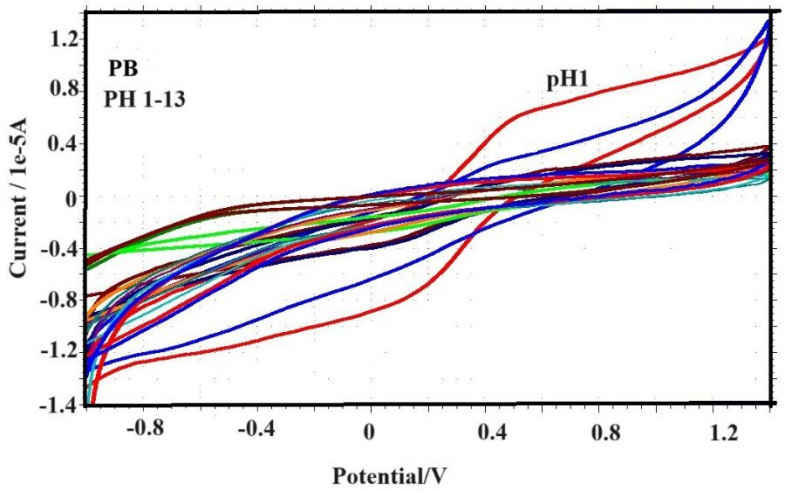

Fig. 4. Cyclic voltammetric responses obtained with a scan rate of 50 mV/s for PB-modified GCE

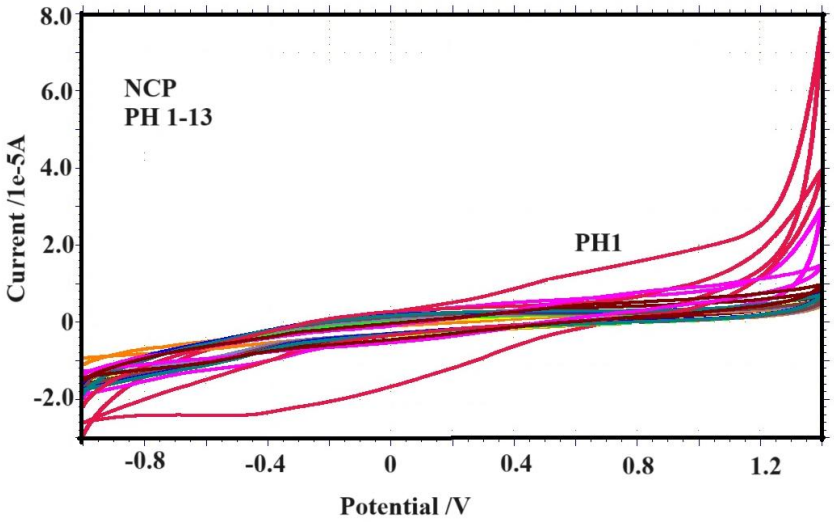

Fig. 5. Cyclic voltammetric responses obtained with a scan rate of 50 mV/s for NCP modified GCE

3.4.2.Effect of concentration:

During the synthesis of NCP, the ORR at 0.2g of ZnO concentration was measured. Fig.6 shows that, when comparing PB and NCP, it is evident that NCP has a greater current peak and an ORR at a lower potential. The XRD and thermal studies further support the optimization of this nanocomposite.

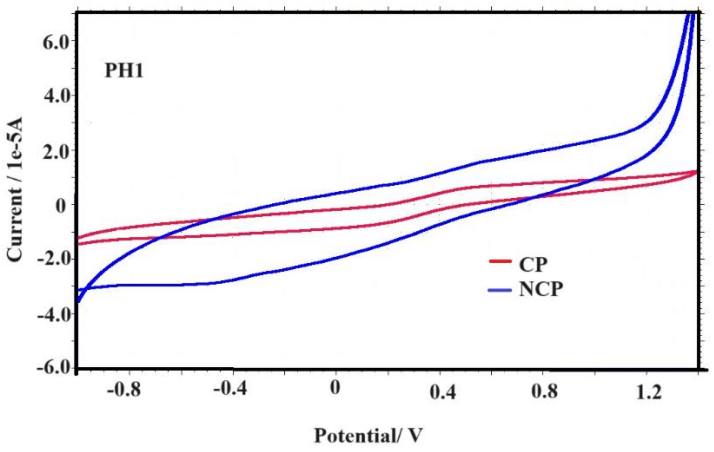

Fig.6.Cyclic voltammetric responses were obtained with a scan rate of 50 mV/s for PB and NCP modified GCE.

3.4.3.Effect of scan rate:

The results of changing the scan rate from 50 mV/s to 500 mV/s are shown in Figs. 7a &8a. The peak current increased as the scan rate increased, indicating that the composite was firmly adhered to the GC electrode surface.

It is noteworthy to note that the CV, which was measured at 500 mV/s, is also well-defined and demonstrates the quick electroactivity of the NCP-modified GCE and PB. As the scan rate was raised, peak potential and peak current both shifted and increased slightly. The current increases slightly linearly, as expected by the equations Y = -0.0032x – 4.0795; R^2 = 0.9954 (for PB) and Y = -0.11391x – 1.36815; R^2 = 0.9970 (for NCP) for the anodic peak currents. This is seen by the plot of logarithm peak current Vs logarithm scan rate in (Figs. 7b and 8b). The polymer's redox process is adsorption-controlled, as indicated by the slope value.[26] The potential scan for the PB& NCP reveals a noticeable peak that indicates the spontaneous nature of the reduction process. This peak is located in the negative voltage (lower side) area. Given that the reduction process would have taken place in the cathode compartment, it may be concluded that PB&NCP are more appropriate for the cathode side. The PB and NCP composites utilized demonstrated efficient electronic conductivity, as demonstrated by the linearly rising current on varying potential scans.
As seen below, the peak current from the Nernstian or reversible systems is determined using the Randles-Sevcik approach (Eq. 4):

$$Ip = 2.69 \times 10^5 \, n^{3/2} A D^{1/2} C \vartheta^{1/2} \qquad \text{……..(4)}$$

Symbols such as Ip, C, A,n, D, and S represent the peak current, concentration (1 M), electrode area (0.071 cm^2), number of transferred electrons (n), diffusion coefficient of the transferred species (D), and scan rate (100 mV/s). Diffusion coefficients for BP and NCP films were found to be $1.0176\times10^{-5}cm^2$ /s and $4.213\times10^{-6}cm^2/s$, respectively. The results obtained showed that the nanocomposite had a greater diffusion coefficient than the copolymer due to the increased electrocatalytic activity of NCP.

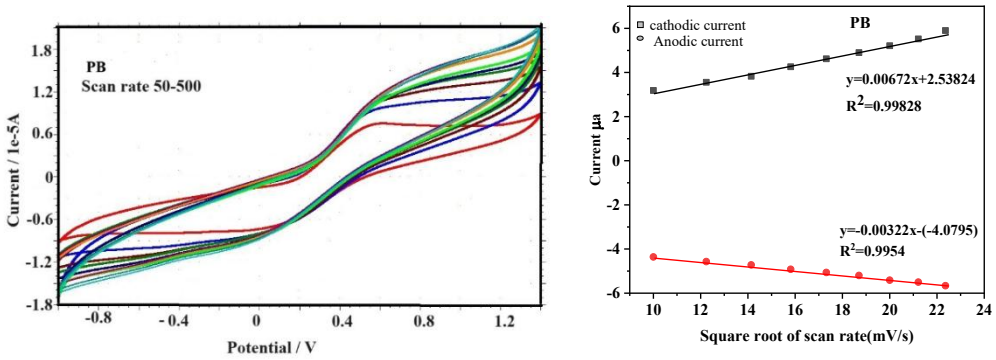

Fig.7. Cyclic voltammetric responses obtained with a scan rate of 50-500 mV/s forPBmodified GCE

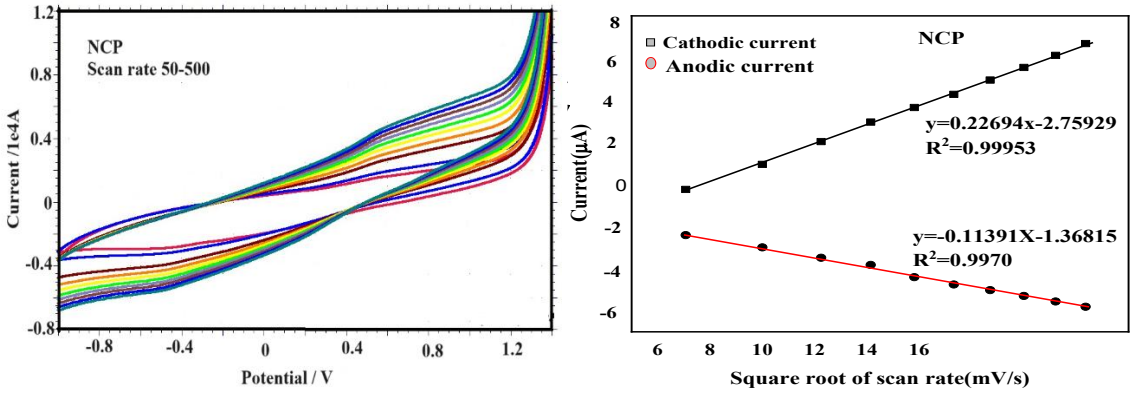

Fig.8. Cyclic voltammetric responses obtained with a scan rate of 50-500 mV/s for NCP modified GCE

3.4.4.Electrochemical behavior of analytes

The benefits of synthesized nanocomposites were first demonstrated by CV (Fig.9). According to the comparison, the typical oxidation peak of ascorbic acid at the NCP nanocomposites (curve c) changed GCE is greater than that at the PB (curve b) modified one. Additionally, when ZnO was added to the nanocomposites, the baseline at the former was noticeably greater than the baseline at the latter. The current responsiveness of NCP nanocomposites (curve c) modified GCE was superior to that of PB. The fact that NCP nanocomposites contain a lot of holes for ascorbic acid-binding could help clarify the phenomenon.

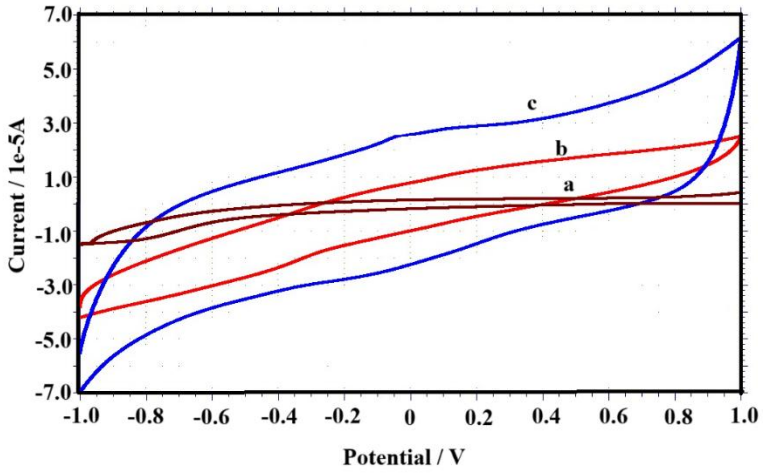

Fig.9. CVs of the a)bare b)PB c) NCP doped GCE in (pH 7) in the presence of AA (0.03mM) at a scan rate of 50 mV/s.

3.4.5. Differential Pulse Voltammetry

The DPV of Ascorbic acid(AA) oxidation on PB and NCP-modified glassy carbon electrodes is presented in Figures 10a&11. The electrocatalytic oxidation of AA was carried out at the PB/GCE and NCP/GCE by varying its concentration from 0.03-0.10 mM.Significant improvement in the magnitude of the anodic electrooxidation response was evident, particularly in the case of PB and NCP modified GCE, which exhibited a strong anodic wave at 0.08V and 0.42.AA concentration ranges in a good linear region in Figure 10 b and 11 b. The AA oxidation linear regression equation was given as I_P=0.50324X+4.26681; R^2=0.99812 for PB and I_P=0.08396X+3.15561; R^2=0.99544.The limit of detection(LOD) and quantification limit (LOQ) were calculated (assumimgS/N=8).LOD for PB and NCP is 1.14mM and 0.44mM.LOQ for PB &NCP is 3.45mm& 1.33 mm by using the formula, LOD=3.3*sb/m, where Sb is the standard deviation of the blank signal and m is the slope of the calibration curve, LOQ=10*sb/m, where Sb is the standard deviation of the blank signal and m is the slope of the calibration curve[27]. It can be concluded that the developed sensor showed good performance in more PB than NCP.

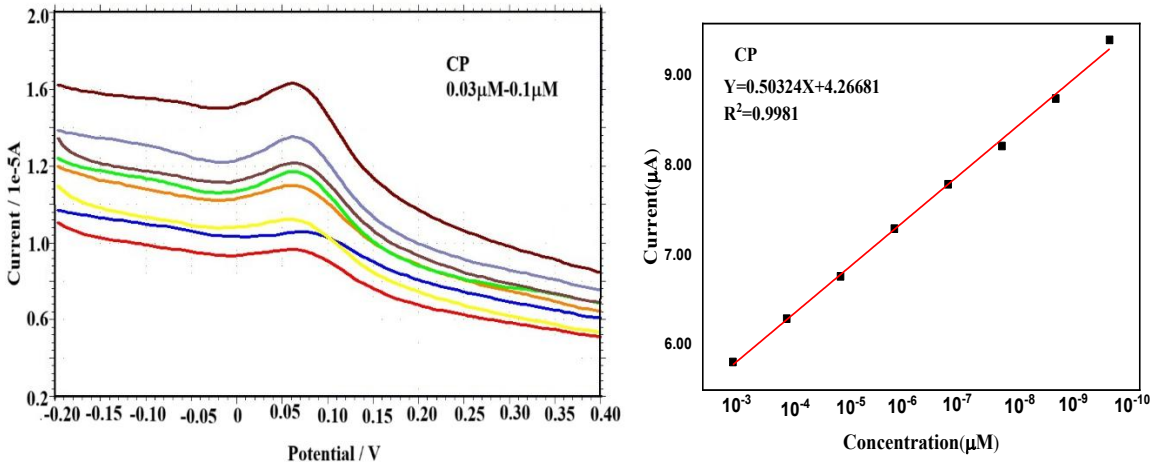

Fig.10a) DPV responses obtained with a scan rate of 100 mV/s for PB modified GCE b) linear plot of PB modified GCE

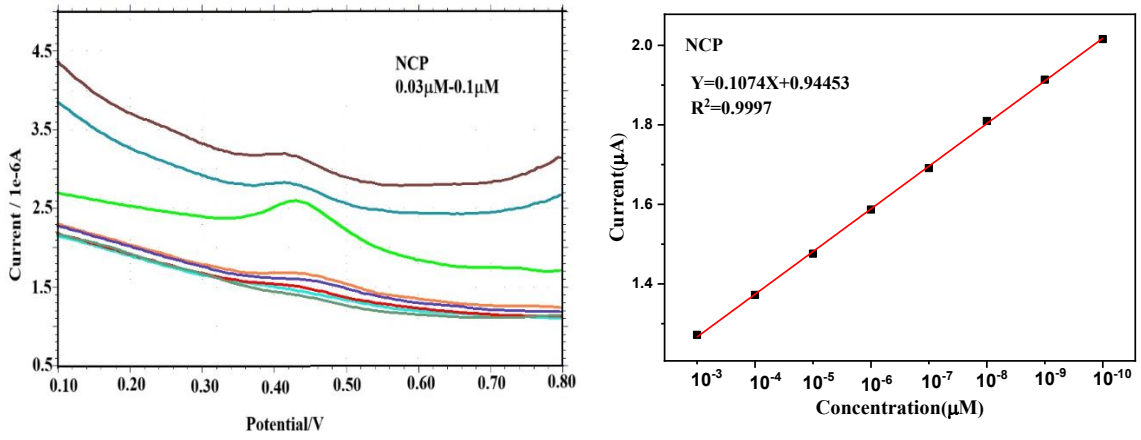

Fig.11 a) DPV responses obtained with a scan rate of 100 mV/s for NCP-modified GCE b) linear plot of NCP modified GCE

4. CONCLUSION

In summary, we have successfully prepared B(PM-PA) and ZnO/B(PM-PA) the nanocomposite via an eco-friendly route and applied it for sensor application. Based on their spectral characterization, the synthesized nanocomposites were determined to incorporate a polymer blend and metal oxide of the composite with greater interaction between them. X-ray diffraction (XRD) structural analyses demonstrated the nanocomposite's semicrystalline structure, with a high average crystallite size of NCP is 11nm. According to CV curves show that these catalysts' current increases from 0.2g ZnO. On the other hand, the NCP-modified electrode exhibited high electrochemical activity towards the detection of AA with the lowest detection limit (LOD) of about 0.44 mM. The benefits of ZnO/B(PM-PA) nanocomposites are demonstrated by the superiority of this novel electrochemical sensor, which has a low detection limit and high current response.

5. ACKNOWLEDGMENTS

The authors are extremely grateful to DST (FAST TRACK and FIST) New Delhi, INDIA for enabling them to utilize the CHI Electrochemical workstation. UV-Vis spectrophotometer at DST-FIST sponsored Department of Chemistry, V.O. Chidambaram College, Tuticorin.

Funding:

This research did not receive any specific grant from funding agencies in the public, commercial, or not-for-profit sectors.

REFERENCES

[1] S.Shrivastava, J.Nimisha, J.Rajeev,"Next-generation polymer nanocomposite-based electrochemical sensors and biosensors",*Trends in Analytical Chemistry*82(2016):55-67.

[2] A.S. Bhattacharyya, "Conducting polymers in biosensing: A review", *Chemical Physics Impact*8(2024):100642-100651.

[3] M.Yuqing, C. Jianrong, X. Xiaohuatitle, "Using electropolymerized non-conducting polymers to develop enzyme amperometric biosensors", *Trends Biotechnol*22(2004): 227-231.

[4] H. Meixner, U. Lampetitle, "Metal oxide sensors",*Sensors and Actuators B: Chemical* 331(1996):198-202.

[5] R. Soumyendu, S.Navneet, B.Reeti, D.S. Misra, A. James, M.C. Laughlin and S.R. Susanta, "Graphene oxide for electrochemical sensing applications", *Journal of Materials Chemistry*21: (2011)14725-14731

[6] L.Gaurav, H.M. Allan,F.Behzad Lin , L.Kasper, F. Kurtis, Q.Xian, M.G.Antonios, G. Balaji, "Two dimensional nanostructure-reinforced biodegradable polymeric nanocomposites for bone tissue engineering", *Biological macromolecules*14(2013): 900–909.

[7] M.M. Josuff Albar, N.A. Jamion, S.N. Atika Baharin, M. Raoov, K.P. Sambasevam, " Preparation of novel commercial polyaniline composites for ammonia detection",*Solid-state phenomena*301(2020):124–131.

[8] H.Christian, H. Richard, S.S. Ulrich, " PMMA based soluble polymeric temperature sensors based on UCST transition and solvatochromic dyes", *Polymer Chemistry*1(2010): 1005–1008.

[9] Z.Chao, G. Saravanan, G. Krishnan, H. YunSuk, Y. Kyusik, "AgNWs-PANI nanocomposite based electrochemical sensor for detection of 4-nitrophenol", *Sensors and Actuators B Chemical*252(2017): 616-623.

[10] W. Yansheng, G. Xiong, L. Yan, "Electrochemical sensors based on polyaniline nanocomposites for detecting Cd(II) in wastewater", *International Journal of Electrochemical Science*19(2024):100519-100525.

[11] S.P.Jong, H.J. Pum, M.P. Kwang, Y. Won-Chol, "Electrochemical Detection of Nitrite on PANI-TiO_2/Pt Nanocomposite–Modified Carbon Paste Electrodes Using TOPSIS and Taguchi Methods", *ACS Omega* 9 (2024): 30583–30593.

[12] N.Shoaie, M. Daneshpour, M. Azimzadeh. S. Mahshid, S.M. Khoshfetrat, F. Jahanpeyma,A.Gholaminejad, K.Omidfar, M. Foruzandeh, " Electrochemical sensors and biosensors based on the use of polyaniline and its nanocomposites: a review on recent advances", *Microchim Acta* 186(2019): 465-472.

[13] J. Yu, T.Huang, Z.Jiang, M. Sun, C. Tang, " Synthesis and Characterizations of Zinc Oxide on Reduced Graphene Oxide for High-Performance Electrocatalytic Reduction of Oxygen", *Molecules* 23(2018): 3227-3232

[14] B. Salma, A. Ayesha,A.Haq Ali Shah, " Highly Selective and Reproducible Electrochemical Sensing of Ascorbic Acid Through a Conductive Polymer Coated Electrode",*Polymers* 11(2019): 1346-1351

[15] J.A.Drisko, J. Chapman, V.J. Hunter, "The use of antioxidants with first-line chemotherapy in two cases of ovarian cancer", *Journal of the American College of Nutrition*22(2003): 118–123.

[16] G.Girma Salale, " Recent advances in electrochemical sensors based on molecularly imprinted polymers and nanomaterials for detection of ascorbic acid, dopamine, and uric acid: A review", *Sensing and Bio-Sensing Research*43(2024): 100610-100615.

[17] W.U. Yiyong, D. Peihong, T. Yaling, F. Jinxia, X. Jingyun, L. Junhua, L. Jun, L. Guangli, H.W. Quanguo, " Simultaneous and sensitive determination of ascorbic acid, dopamine, and uric acid via an electrochemical sensor based on PVP-graphene composite",*Journal of Nanobiotechnology*18 (2020):11-15

[18] S.H. Abu Hassan, M.M. Ramli, M. Abdullah, M.N. Mohtar, N.A. Rahman, A. Ahmad, N.H. Osman, F. Rusydi, "Effects of Polymerization Time towards Conductivity and Properties of Poly(methyl methacrylate)/ Polyaniline (PMMA/PANi) Copolymer", *Sustainability* 14 (2022) :8940-8948

[19] S.Angappane, N. Rajeev Kini, T.S. Natarajan, G. Rangarajan, B.Wessling, " PAni–PMMA blend metal Schottky barriers" *Thin Solid Films* 417 (2002):202–205

[20] M.M. Abutaliba, "Insights into the structural, optical, thermal, dielectric, and electrical properties of PMMA/PANI loaded with graphene oxide nanoparticles" *Physica B Condensed Matter* 552(2019):19–29

[21] Z.H. Fatma, N. Nacira, "Improvement of the structural and electrical properties of PMMA/PANI-MA blends synthesized by interfacial in situ polymerization in a continuous organic phase", *Polymer Bulletin* 79 (2022): 37–63

[22] Y.T.Mohamed, S. Adel, B. Cherifa, B. Ahmed, "Synthesis of Polyaniline-Zinc Oxide Composites: Assessment of Structural, Morphological, and Electrical Properties", *Annales de Chimie-Sciences des Materiaux* 47 (2023):

399-404

[23] J. Shanavas Khan, R. Asha, B. Beena, " Polyaniline/Zinc Oxide Nanocomposite as a Remarkable Antimicrobial Agent in Contrast with PANI and ZnO", *Indian Journal of Adances in Chemical Science* 6(2018) : 71-76.

[24] S. Devikala, P. Kamaraj, M. Arthanareeswari, "Conductivity and Dielectric Studies of PMMA Composites", *Chemical Science Transactions* 2(2013): S129-S134

[25] B.Salma, A. Ayesha, A.S. Anwar-ul-Haq, "Highly Selective and Reproducible Electrochemical Sensing of Ascorbic Acid Through a Conductive Polymer Coated Electrode", *Polymers* 11(2019): 1346-1352.

[26] L.L.Israel, K. Sutripto, M.W. Lodrick, E.F. Olu, " Polypyrrole@polyaniline-reduced graphene oxide nanocomposite support material and Cobalt for the enhanced electrocatalytic activity of nickel phosphide microsphere towards alkaline urea oxidation", *Materials Research Express* 8(2021) :095303-095315

[27] F. Zina, B.A.Mounir, N.A.Mohammed, D. Eithne, "Simultaneous determination of ascorbic acid, uric acid and dopamine using silver nanoparticles and copper monoamino-phthalocyanine functionalised acrylate polymer", Analytical Methods 12(2020): 3883-3891